Purdue University
Purdue e-Pubs

International Refrigeration and Air Conditioning Conference | School of Mechanical Engineering

2004

Analysis of Two-Phase Flow in Double-Pipe Condensers and Evaporators With Special Emphasis on Transition Zones: Numerical Model and Experimental Comparison

Joaquim Rigola
Universitat Politecnica de Catalunya

Sergio Morales
Universitat Politecnica de Catalunya

Gustavo Raush
Universitat Politecnica de Catalunya

Carlos D. Perez Segarra
Universitat Politecnica de Catalunya

Follow this and additional works at: http://docs.lib.purdue.edu/iracc

Rigola, Joaquim; Morales, Sergio; Raush, Gustavo; and Segarra, Carlos D. Perez, "Analysis of Two-Phase Flow in Double-Pipe Condensers and Evaporators With Special Emphasis on Transition Zones: Numerical Model and Experimental Comparison" (2004). *International Refrigeration and Air Conditioning Conference.* Paper 658.
http://docs.lib.purdue.edu/iracc/658

This document has been made available through Purdue e-Pubs, a service of the Purdue University Libraries. Please contact epubs@purdue.edu for additional information.
Complete proceedings may be acquired in print and on CD-ROM directly from the Ray W. Herrick Laboratories at https://engineering.purdue.edu/Herrick/Events/orderlit.html

ANALYSIS OF TWO-PHASE FLOW IN DOUBLE-PIPE CONDENSERS AND EVAPORATORS WITH SPECIAL EMPHASIS ON TRANSITION ZONES: NUMERICAL MODEL AND EXPERIMENTAL COMPARISON

Joaquim RIGOLA, Sergio MORALES, Gustavo RAUSH, Carlos D. PÉREZ-SEGARRA

Centre Tecnològic de Transferència de Calor CTTC,
Laboratori de Termotècnia i Energètica,
Dept. Màquines i Motors Tèrmics. Universitat Politècnica de Catalunya,
Colom 11, 08222 Terrassa (Barcelona), Spain
Fax: +34-93-739.89.20, Tel. +34-93-739.81.92
E-mail: labtie@labtie.mmt.upc.es, Web page: http://www.cttc.upc.edu

ABSTRACT

A numerical study of the thermal and fluid-dynamic behavior of the two-phase flow in conducts is presented. The numerical simulation has been developed by means of the finite volume technique based on a one-dimensional transient integration of the conservative equations. The discretized governing equations are solved using the step by step algorithm or the pressure-based method SIMPLEC, giving special emphasis on the treatment of the transition zones between the different phases. The numerical comparative results show the verification of the numerical model developed, while the experimental comparative results validate the simulation and show the improvements in the solution when the special treatment is used. A experimental unit has been designed and built to analyse single stage vapour compression refrigerating equipment and to compare the whole refrigerating system numerically. A detailed instrumented evaporator has been added in order to obtain the experimental information of temperature and pressure distribution along the heated duct. The electrically heated instrumented evaporator has given detailed experimental data to be compared with the numerical results.

1. INTRODUCTION

The thermal and fluid-dynamic behavior of the fluid refrigerants inside the heat exchanger in condensation and evaporation processes present different phenomena. The quick change of the heat transfer coefficient and friction factor from one region to another, together with the necessity of using new non-contaminant refrigerants are important reasons for the study and research on this topic. The numerical simulation model and its improvements are a strong tool for design and optimization of these thermal equipments.

This paper is focused on a detailed one-dimensional numerical simulation of phase change phenomena within tubes. The discretized governing equations are coupled, and the resolution can be obtained by means of two different methods. The first manner is a fully implicit step by step method in which the continuity, momentum and energy equations are solved together at each control volume in the flow direction (Escanes et al., 1995) and (García-Valladares et al., In Press). The second manner is a fully implicit segregated pressure-based method SIMPLE (Patankar, 1980) based on the sequential resolution of the all field. Different numerical aspects have been evaluated with the aim of verifying the quality of the numerical solution. Convergence errors, discretization errors, resolution comparison algorithm and numerical schemes are also evaluated.

The mathematical formulation requires the use of empirical information for the evaluation of the void fraction, heat transfer coefficient, shear stress and friction factor in the tubes. Different empirical correlations have been selected for condensation and evaporation cases. The numerical results have been obtained considering R134a as fluid refrigerant, while all properties have been evaluated by means of the REPROP properties program (NIST, 1996). A detailed experimental comparison between numerical model and literature in heat exchangers has been performed using (Cavallini et al., 2001) and (Kattan et al., 1998a).

A numerical simulation and a description of the compression refrigerating equipment (Rigola et al., 2003), extended with the detailed instrumented evaporator and the experimental validation is shown, together with extensive illustrative experimental comparative results. The unit studied consists of a hermetic reciprocating compressor, a double-pipe condenser and evaporator, a specific instrumented electrically heated pipe evaporator, an expansion device and the different tube connections. The attention has been focused on the detailed instrumented evaporator. In this element, solid wall and fluid flow temperatures, together with pressure distribution are experimentally obtained and numerically compared with the numerical model.

2. MATHEMATICAL FORMULATION

The mathematical formulation of the two phase flow inside a characteristical control volume, and the hypothesis assumed in the numerical model, together with the heat conduction in internal tube wall are presented in (García-Valladares et al., In Press). The government equations are composed by continuity, momentum and energy. The shear stress in the momentum equation and the heat transfer coefficient in the energy equation are defined by means of the empirical information for single or two-phase flow.

3. EMPIRICAL INFORMATION

The empirical information needed in single phase and two phase are presented. The single phase heat transfer coefficient is calculated using Nusselt and Gnieliski correlations (Amstrong, R.C., 1983), for laminar and turbulent regimes, respectively, while the friction factor is evaluated from the Churchill expression (Amstrong, R.C., 1983).

A two phase flow region have two different processes: condensation and evaporation. The heat transfer coefficient for condensation can be evaluated from two different correlations. The Dobson and Chato correlation (Dobson and Chato, 1998) allows to calculate the heat transfer coefficient on annular or wavy flow. Shah correlation for condensation (Shah, 1979) is specific for annular flow. The empirical correlation presented above is available for weight fraction between 0.15 to 0.85, for the rest of the range there is no data available. In this case, the heat transfer coefficient has to be extrapolated between the single phase region and two phase region. The Shah correlation by condensation has been adapted considering continuity and derivability between single-phase and two phase.

Three sub-zones are presented inside the evaporation when a two phase flow appears. These sub-zones are subcooled boiling, saturated boiling and dryout. The heat transfer coefficient for evaporation can be evaluated from different correlations depending on which sub-zone is the flow. The heat transfer coefficient in the subcooled zone is determined by Forter and Zuber correlation (Amstrong, R.C., 1983) or Kandlikar subcooling correlation (Kandlikar, 1991). Theses correlation can be used when the wall temperature at a given location must be equal to or greater than the local saturated temperature. The heat transfer for the saturated zone is evaluated by Shah correlation for saturated boiling (Shah, 1982), Kandlikar correlation for saturated flow boiling (Kandlikar, 1998) or Kattan correlation (Kattan et al., 1998a). The heat transfer coefficient in the dryout zone is calculated by Kattan correlation (Kattan et al., 1998b) and (Kattan et al., 1998c) or Groeneveld correlation (Groeneveld, 1973). The Groneveld correlation requires to determine a previous point where the dryout condition begins, while the Kattan correlation estimates and recognizes the dryout point by means of the evaporation flow pattern maps.

The void fraction is calculated from the semi-empirical equation (Rice, 1987). In a two phase flow, the shear stress is determined by means of the friction factor gas f_g, gas mass flux $\dot{m}_g$, gas density ρ_g and the multiplier two phase factor. The friction factor and multiplier two phase factor are empirically calculated by the Jung correlation (Jung and Radermacher, 1993) or the Friedel correlation (Friedel, 1979).

4. NUMERICAL SOLUTION

The discretization of government equations and the convergence criteria used in this numerical model are detailed in (García-Valladares et al., In Press). Other aspects are presented in this section, such as boundary conditions, schemes and the treatment between the transition zones.

4.1 Initial and boundary conditions

At the initial instant, the fluid pressure, mass flux and enthalpy distribution along all tube control volume CVs, together with tube temperature, must be specified. The Step by Step method needs to know the inlet mass flux $\dot{m}_i$, pressure p_i and enthalpy h_i. When the SIMPLEC method is used, the inlet mass flux $\dot{m}_i$, enthalpy h_i, and the outlet pressure p_o, must be specified.

4.2 Numerical schemes

Convective terms are evaluated by means of the first-order Upwind scheme or high order scheme, such as central different CDS, Quick or Smart schemes. All these schemes are used within the two different resolution algorithms. Thus, the step by step method considers Upwind or CDS scheme, while the pressure-based method SIMPLE works with Upwind, Quick or Smart scheme.

4.3 Differentiation between regions

The transition criteria between the three main regions existing in both condensation and evaporation processes are evaluated depending on fluid enthalpy. These conditions are: i) liquid region: the value of the enthalpy at the outlet control volume h_o is lower than the liquid saturation enthalpy $h_{l,sat}$. ii) two phase region: the enthalpy at the outlet control volume h_o is greater than the liquid saturation enthalpy $h_{l,sat}$ and is lower than the gas saturation enthalpy $h_{g,sat}$. iii) gas region: the enthalpy at the outlet control volume h_o is greater than the gas saturation enthalpy $h_{g,sat}$. The evaporation processes have two subzones or subregions: sub-cooled boiling and dryout. The sub-cooled boiling criteria begins when the fluid enthalpy h is lower than the saturation enthalpy of liquid $h_{l,sat}$ and the wall temperature T_{wall} is greater than the saturation temperature of fluid T_{sat}. The dryout criteria begins when the fluid enthalpy h is lower than the saturation enthalpy of gas $h_{g,sat}$, but is greater than the saturation enthalpy of liquid $h_{l,sat}$, and if the weight fraction x_g is greater than the weight fraction for dryout $x_{g,do}$.

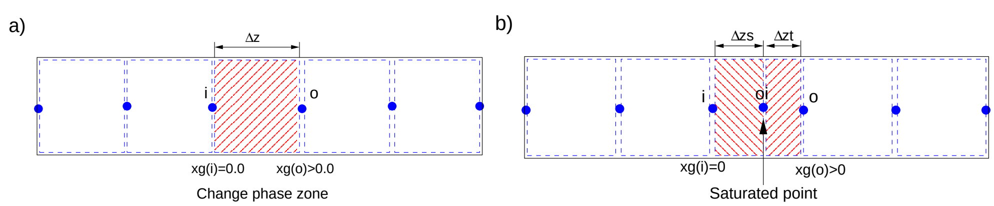

Figure 1: Transition between regions. a) CV where the transition occurs, b) CV divide in two parts.

Using the previous conditions at each control volume, it is possible to define the work region. The control volume where transition between region occurs is divided in to two control volumes, as depicted in Figure 1. The length of the first part of the volume is calculated from the energy equation, imposing a saturation condition at the outlet, and momentum and mass equations are solved as single phase. In the second part of the control volume momentum, mass and energy equations are solved as two phase. The transition from two phase to single phase is solved in the same way.

5. NUMERICAL RESULTS

The numerical results using step by step and SIMPLEC algorithms are detailed in Table 1, where the numerical results depending on accuracy desired and density mesh considered. The goal of this section is to show the quality of the numerical solution by means of a critical analysis of the different numerical sources of computational errors: convergence, discretization, and programming error. Results show how global numerical values tend to give an asymptotic solution, this solution is independent of the mesh density and accuracy desired.

Table 1: Numerical study using the Step by Step and Simplec method

Step by Step method				Simplec method			
Precision	p_{out} (kPa)	h_{out} (kJ/kg)	$\dot{Q}_{out}$ (W/m^2)	Precision	p_{out} (kPa)	h_{out} (kJ/kg)	T_{out} (^oC)
10^{-2}	1047.6514	255.6866	60803.2478	10^{-6}	1039.0020	230.0065	21.7789
10^{-4}	1047.6503	255.6945	60803.5030	10^{-8}	1039.0020	230.0044	21.7774
10^{-6}	1047.6503	255.6945	60803.4939	10^{-9}	1039.0020	230.0044	21.7774
10^{-8}	1047.6503	255.6945	60803.4936	10^{-10}	1039.0020	230.0044	21.7774
Grid Size	p_{out} (kPa)	h_{out} (kJ/kg)	$\dot{Q}_{out}$ (W/m^2)	Grid Size	p_{out} (kPa)	h_{out} (kJ/kg)	T_{out} (^oC)
200	1047.6514	255.6866	60782.7427	200	1039.0162	230.2771	21.971
400	1047.6503	255.6945	60795.1112	400	1039.0081	230.1232	21.862
800	1047.6503	255.6945	60800.2449	800	1039.0040	230.0441	21.806
1600	1047.6503	255.6945	60803.4936	1600	1039.0020	230.0044	21.777

When the Step by Step method is used values between $10e{-4}$ and $10e{-8}$ in accuracy produce a difference around 0.0000155% in heat flux $\dot{Q}_{out}$, and do not report difference in pressure and enthalpy. The influence of the mesh density can been see when value between 200 and 1600 in the mesh density produce a difference approximately 0.000105% in pressure p_{out}, approximately 0.00308% in enthalpy h_{out} and approximately 0.0341% in heat flux $\dot{Q}_{out}$. The asymptotic solution is considered as a case with 1600 CV and precision value of $10e^{-8}$.

The Simplec method produce difference approximately 0.00091% in enthalpy h_{out}, approximately 0.00688% in temperature t_{out} and do not report difference in pressure, when values between $10e{-6}$ and $10e{-10}$ accuracy are used. The influence of the mesh density is evaluated, and values between 400 and 1600 in the mesh density ia approximately 0.000587% in pressure p_{out}, approximately 0.0516% in enthalpy h_{out} and approximately 0.390% in temperature t_{out}. The asymptotic solution is considered as a case with 1600 CV and precision value of $10e^{-10}$.

6. EXPERIMENTAL COMPARISON

A comparison has been carried out from experimental results obtained through scientific literature. Two different cases are presented.

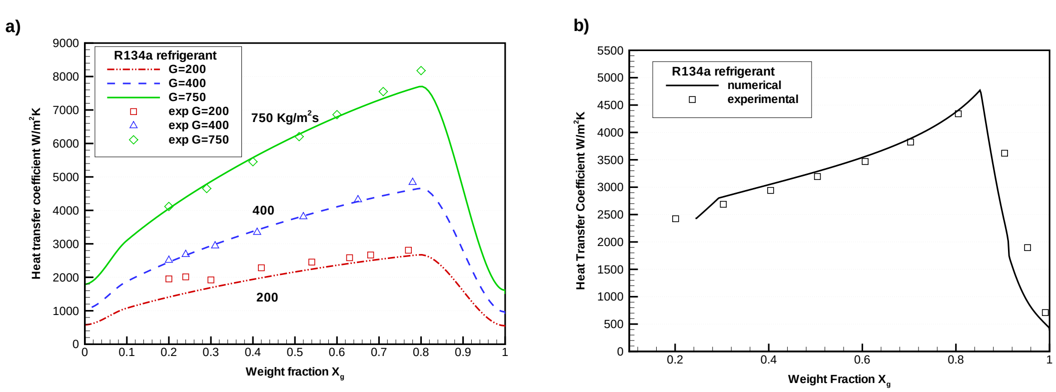

Figure 2: Comparison of the numerical solution and experimental data. a) Condensation, b) Evaporation.

6.1 Condensation

The numerical simulation of the condensation process has used the adapted treatment of the heat transfer coefficient correlation. Validation is obtained by means of the comparison between the numerical results and experimental data of Cavallini (Cavallini et al., 2001). Cavallini reported the experimental heat transfer coefficient for condensation inside an 8 mm diameter tube with mass flux 200, 400 and 750 kg/m^2s of the refrigerant R134a. The comparison between the numerical and experimental data in condensation is depicted in Figure 2a. With a mass flux of 400 and 750 kg/m^2s, the numerical results are very similar to the experimental data, when the mass flux of 200 kg/m^2s is used, the numerical result under-predicts the experimental data. The results with adapted treatment correlation do not produce abrupt alterations in the value of the heat transfer coefficient and gives stability to the numerical resolution process.

6.2 Evaporation

Kattan (Kattan et al., 1998a) reported the experimental heat transfer coefficient in the evaporation of the R134a. The evaporation occurs at 10 ^oC of saturated temperature inside a 12 mm diameter tube, and a mass flux of 200 kg/m^2s. A constant heat flux of 10000 W/m^2 is applied to the tube. The comparison between the numerical simulation and the experimental data of heat transfer coefficient is depicted in Figure 2b. A good behaviour of numerical simulation is showed and the heat transfer coefficient change next to a dryout point is detected. This case has more difficult problems with the quick change of the heat transfer coefficient at a dryout point. When the Kattan correlation is used and the differentiation between regions technics is applied, the problem was solved and the solution for cases that include post-dryout can now be simulated.

7. EXPERIMENTAL SETUP

An experimental unit has been built to study single stage vapour compression refrigerating systems. A schematic diagram of the experimental unit and the detailed evaporator added is depicted in Figure 3 and a picture of the refrigeration system is showed in Figure 4.

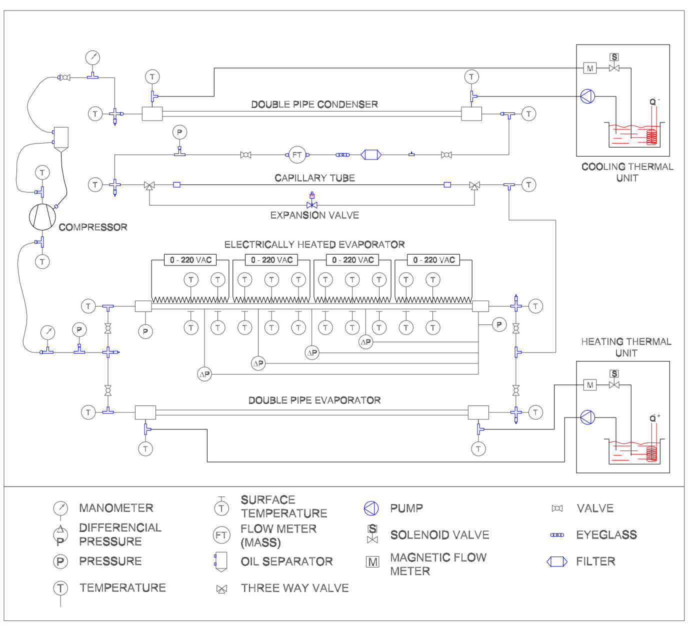

Figure 3: Schematic representation of the instrumented unit.

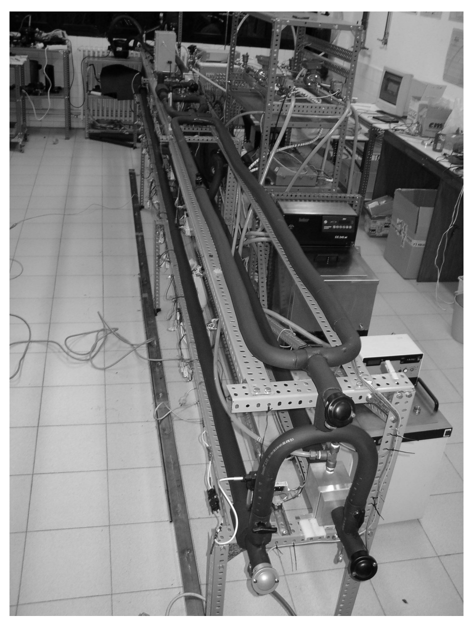

Figure 4: Top general view of the refrigeration system.

Elements that make up the experimental unit are: a hermetic reciprocating compressor, double pipe condenser and evaporator, electrically heated evaporator, together with an expansion valve. The auxiliary fluid used in the double pipe condenser and evaporator annul is water. The fluid flow temperature inside tubes and annul are measured with platinum resistance Pt-100 thermometer sensors, located at the inlet and outlet sections of each element of the main and second circuits.

Condenser and evaporator absolute pressures are measured by transducers in ranges of bars 0-16 and 0-6 bars, respectively. Pressure transducers accuracy is ±0.05% F.S. Refrigerant mass flow rate is measured with a Coriolis-type mass flow-meter with an accuracy of ±0.0009 kg/min. Two thermostatic heating and cooling units control the inlet auxiliary water temperature in the condenser and evaporator auxiliary circuits, respectively. The volumetric flow in these secondary circuits is controlled by two modulating solenoid valves and measured by means of two magnetic flow-meters, with an accuracy of ±0.01 l/min. from 0 to 2.5 l/min., and ± 0.5% F.S. from 2.5 l/min. to 25 l/min.

Under the initial experimental conditions, the single stage cycle is working with the double-pipe heat exchangers, without the electrically heated evaporator. Once the working conditions are obtained and the steady state conditions are reached, the mass flow is gradually changed from the double pipe evaporator to the electrically heated evaporator with equal heat exchanged, in order to obtain the same conditions independently while the evaporator is working.

8. DETAILED INSTRUMENTED EVAPORATOR

The test section is a copper tube of a length of 6 m with a 0.00965 m diameter. At the inlet and outlet evaporator cross section, 2 platinum resistance Pt-100 sensors measure the fluid flow temperature. The rest of the fluid temperatures along the tube are measured with 10 calibrated K-type thermocouples with an accuracy of ±0.2^{o}C. These thermocouples are encapsulated inside a thin steel stick of a diameter of 0.25 mm, and are located at different points from the inlet to the outlet sections in the centre of the round tube. The external wall pipe temperatures are measured by means of 20 wall K-type thermocouples stuck at the top and bottom external wall along the evaporator tube. The external wall thermocouples have also an accuracy of ±0.2^{o}C.

The tube has been electrically heated with 6 wired electrical resistances each with an electrical power of 200W. The electrical resistances are individually controlled by a Field-Point National Instruments PWMs (Pulse Width Modulators). The evaporator has been tested dividing its 6 m of length in 6 different parts and individually controlled. The accuracy on the absorbed power values is less than 1%.

The absolute pressure is measured by two transducers at the inlet and outlet cross section of the evaporator. Both transducers have a range of 0-6 bars, with an accuracy within ± 0.05% F.S. By means of capillary tubes, 4 points along the evaporator are instrumented to obtain the differential pressure between these points and the outlet cross section. A differential pressure transducer is used with an accuracy of ± 0.05% F.S.

9. EXPERIMENTAL RESULTS

The experimental results obtained under steady state conditions in the overall cycle system, when the double pipe evaporator is working instead of the electrically heated are showed in Table 2.

Table 2: Experimental values of the whole cycle variables

case 1				case 2				case 3			
T_{iev} $[^oC]$	p_{iev} $[bar]$	$\dot{m}$ $[kg/h]$	$\dot{Q}$ $[W]$	T_{iev} $[^oC]$	p_{iev} $[bar]$	$\dot{m}$ $[kg/h]$	$\dot{Q}$ $[W]$	T_{iev} $[^oC]$	p_{iev} $[bar]$	$\dot{m}$ $[kg/h]$	$\dot{Q}$ $[W]$
17.50	1.26	4.73	227	20.11	1.95	7.69	450	21.80	2.69	10.95	660

Information in table represent the fluid temperature T_{iev}, and pressure p_{iev} at the inlet, mass flux $\dot{m}$ and heat adsorbed $\dot{Q}$ in evaporator. Once the results are obtained, the heat absorbed in the evaporator is the same as the heat electrically rejected by the instrumented evaporator.

Experimental results over the evaporator instrumented are detailed in Table 3, where fluid temperature T_f, top wall temperature T_{w-T}, bottom wall temperature T_{w-B} and pressure p in evaporator to different length are showed. The electrical heat is divided in 6 zones where different power are absorbed at each evaporator meter from the inlet cross section to the outlet cross section, respectively. The total heat exchanger in the instrumented evaporator is similar than the heat exchanged in the double pipe evaporator.

Table 3: Experimental values through the electrically heated evaporator

Evap.	case 1				case 2				case 3			
length	T_f	T_{w-T}	T_{w-B}	p	T_f	T_{w-T}	T_{w-B}	p	T_f	T_{w-T}	T_{w-B}	p
$[m]$	$[^oC]$	$[^oC]$	$[^oC]$	$[bar]$	$[^oC]$	$[^oC]$	$[^oC]$	$[bar]$	$[^oC]$	$[^oC]$	$[^oC]$	$[bar]$
0.0	-21.92			1.2610	-11.5			1.9528	-3.14			2.6967
0.75	-19.58	-17.65	-17.87		-10.81	-7.71	-7.97		-2.58	0.44	0.14	
1.25	-19.58	-17.60	-17.33		-10.81	-8.08	-7.37		-2.58	0.22	1.43	
1.75	-19.18	-18.55	-17.80		-10.74	-8.58	-7.30		-2.51	0.35	2.38	
2.00				1.2537				1.9401				2.6878
2.25	-20.93	-18.18	-17.57		-10.65	-7.33	-6.19		-2.42	1.35	2.98	
2.75	-20.93	-18.60	-17.14		-10.65	-8.16	-5.5		-2.42	0.06	3.78	
3.00				1.2476				1.9298				2.6690
3.25	-20.72	-16.96	-17.43		-10.60	-6.67	-7.56		-1.78	2.07	1.12	
3.75	-8.61	11.79	11.28		-8.79	4.57	3.49		-0.35	3.26	0.87	
4.00				1.2435				1.9234				2.6551
4.25	5.67	23.53	23.56		5.16	29.53	29.58		8.89	32.53	32.93	
4.75	18.57	33.93	33.94		20.60	41.78	41.86		22.59	43.45	43.58	
5.00				1.2414				1.9200				2.6457
5.25	29.56	41.89	41.43		33.97	51.97	51.11		35.10	55.26	54.03	
6.00	43.41			1.2404	51.71			1.9199	53.71			2.6411

The experimental results show how the evolution of the fluid temperature is constant until the dry out point, after that the single phase fluid flow quickly increase. The wall temperature evolution has no abrupt changes, and it has the same evolution as the fluid flow temperature. Finally, the fluid pressure evolution is almost linear along all evaporator pipe.

10. DETAILED COMPARISON

The experimental illustrative cases presented above are numerically compared with the model presented. Three heat transfer correlations for evaporation phenomena are numerically compared and experimentally validated in these cases. Three more different friction factor correlations are also used in this detailed comparison.

Figure 5 shows the comparative results of the fluid temperature distribution, the wall temperature, pressure and heat transfer coefficient for all cases. Very good agreement between numerical results and experimental data is obtained. The three friction factor correlations show the same numerical results. Comparative results between numerical results and experimental data show the same pressure drop evolution, although numerical results are overestimated around 0.3% in all compared points along the evaporator.

The most important difference between the three correlations is in the wall temperature comparison. The Kattan correlation clearly shows the most agreement comparison. The other correlations do not take into account the real transition evolution of the heat transfer coefficient from the two-phase flow and dry-out to a single vapour phase. The experimental wall evolution shows that there are no abrupt changes, and the fluid flow and wall temperature have the same evolution along the evaporator pipe. In conclusion, the

Kattan correlation is the heat transfer model that shows the best agreement between the numerical results and experimental data.

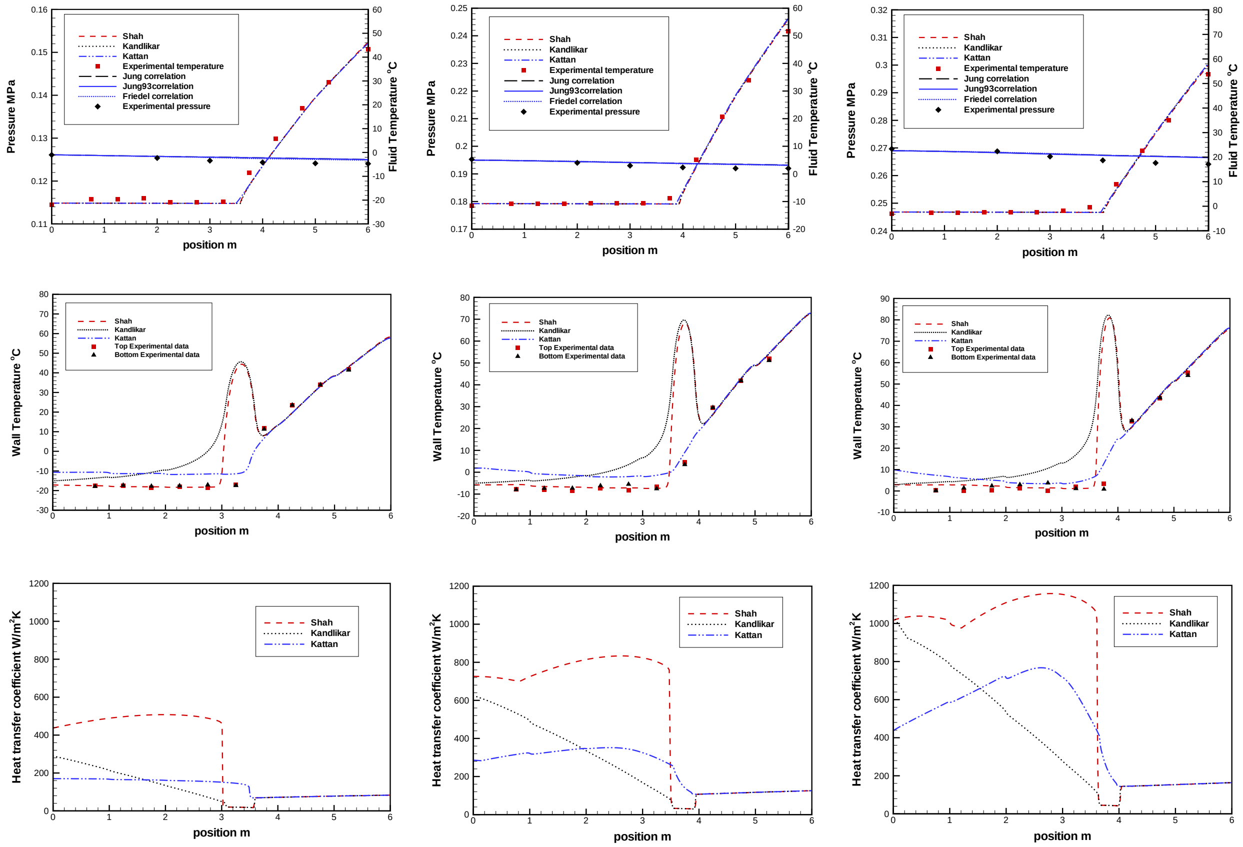

Figure 5: Fluid and wall temperature, pressure and heat transfer coefficient

11. CONCLUSIONS

A numerical model for analyzing the condensation and evaporation inside ducts by means of a transient one-dimensional analysis of fluid flow has been presented. The Step by Step and SIMPLEC method have been used to resolve the conservation equations in single phase and two phase. A numerical study has been shown to verify the numerical model. The quality of the numerical solution has been assessed by means of a critical analysis of the different numerical source of errors. The results make the influence of different numerical parameters clear: convergence criteria, number of grid nodes, numeric schemes, etc., in order to obtain solutions not dependent on numerical parameters chosen.

The step by step method is much faster than the SIMPLEC method in the resolution process and the result obtained with the two methods is similar. The adapted treatment for the heat transfer coefficient correlation and criteria of the transition zones gives a robust characteristic of convergence to the numerical process, and does not affect the value of the variables in the fluid.

The detailed instrumentation in evaporator has allowed to compare the fluid flow and pressure drop distribution, together with the wall pipe temperature evolution along the tube. Comparative results have shown the good agreement in the pressure drop and fluid flow distribution. However, the most important discrepancies are presented in the wall tube temperature and heat transfer coefficient evolution. The Kattan correlation, the only one which takes into account the evolution from two-phase to dry-out and single phase, shows a more realistic wall temperature distribution.

REFERENCES

Amstrong, R.C., 1983, *Heat Exchanger Design Handbook HEDH*, volume 2, Hemisphere, NY, USA.

Cavallini, A., Censi, G., Del Col, D., Doretti, L., G.A., L., and Rossetto, L., 2001, Experimental Investigation on Condensation Heat Transfer and Pressure Drop of New HFC Refrigerants (R134a, R125, R32, R410A R236ea) in a Horizontal Smooth Tube, *International Journal of Refrigeration*, 24:p. 73–87.

Dobson, M. and Chato, J., 1998, Condensation in Smooth Horizontal Tubes, *Journal of Heat Transfer, Transaction of ASME*, 120:p. 193–213.

Escanes, F., Pérez-Segarra, C., and Oliva, A., 1995, Thermal and Fluid-Dynamic Behaviour of Double-Pipe Condenser and Evaporators, A Numerical Study, *International Journal of Numerical Methods for Heat and Fluid Flow*, 5, no. 9.

Friedel, F., 1979, Improved Friction Pressure Drop Correlation for Horizontal and Vertical Two-Phase Pipe Flow, *European Two-Phase Flow Group Meeting*, Ispra, Italy. Paper E2.

García-Valladares, O., Pérez-Segarra, C., Rigola, J., and Oliva, A., 1998, Detailed numerical simulation of condensers and evaporators using pure and refrigerant mixtures, *International Compressor Engineering Conference*, Purdue University, IN, USA, p. 201–206.

García-Valladares, O., Pérez-Segarra, C., Rigola, J., In Press, Numerical Simulation od Doble-pipe Condesers and Evaporators, *International Journal of Refrigeration*.

Groeneveld, D., 1973, Post-Dryout Transfer at Reactor Operating Conditions, *ANS Conference No. 730304*, p. 321–350.

Jung, D. and Radermacher, R., 1993, Prediction Heat Transfer Coefficient and Pressure Drop of Refrigerant Mixtures in Horizontal Tubes, *International Journal of Refrigeration*, 16, no. 3:p. 201–209.

Kandlikar, S., 1991, Development of a Flow Boiling Map for Subcooled and Saturated Flow Boiling of Different Fluid Inside Circular Tubes, *Journal of Heat Transfer*, 113:p. 190–200.

Kandlikar, S., 1998, Heat Transfer Characteristics in Partial Boiling, Fully Developed Boiling and Significant Void Flow Regions of Subcooled Flow Boliling, *Journal of Heat Transfer*, 120:p. 395–399.

Kattan, N., Thome, J., and Fravrat, D., 1998a, Flow Boiling in Horizontal Tubes: Part I - Development of a Diabatic Two-Phase Flow Pattern map, *Journal of Heat Transfer*, 120:p. 140–147.

Kattan, N., Thome, J., and Fravrat, D., 1998b, Flow Boiling in Horizontal Tubes: Part II - New Heat Transfer Data for Five Refrigerants, *Journal of Heat Transfer*, 120:p. 148–155.

Kattan, N., Thome, J., and Fravrat, D., 1998c, Flow Boiling in Horizontal Tubes: Part III - Development of a New Heat Transfer Model Based on Flow Pattern, *Journal of Heat Transfer*, 120:p. 156–165.

National Institute of Standards and Technology NIST, 1996. REFPROP v.5.0, NIST Thermodynamic Properties of Refrigerants and Refrigerant Mixtures Database. Gaithersburg, MD, USA.

Patankar, S., 1980, *Numerical heat transfer and fluid flow*, McGraw-Hill.

Rice, C., 1987, The effect of Void Fraction Correlation and Heat Flux Assumption on Refrigerant Charge Inventory Predictions, *ASHRAE Transaction*.

Rigola, J., Pérez-Segarra, C., and Oliva, A., 2003, Modeling and numerical simulation of the thermal and fluid dynamic behavior of hermetic reciprocating compressors. Part 2: Experimental investigation., *International Journal of Heating, Ventilating, Air-Conditioning and Refrigerating Research*, 9, no. 2:p. 237 – 250.

Shah, M., 1979, A General Correlation for Heat Transfer During Film Condensation Inside Pipes, *International Journal Heat Mass Transfer*, 22:p. 547–556.

Shah, M., 1982, Chart Correlation for Saturated Boiling Heat Transfer: Equations and Further Study, *ASHRAE Transaction*, , no. 88.

ACKNOWLEDGEMENTS

The authors gratefully acknowledge the financial support provided by the Comisión Interministerial de Ciencia y Tecnología (ref. n^o. TIC2003-07970).